



HAL
open science

Generation of a C57BL/6J mouse strain expressing the CD45.1 epitope to improve hematopoietic stem cell engraftment and adoptive cell transfer experiments

Daphné Laubretton, Sophia Djebali, Céline Angleraux, Benny Chain, Maxence Dubois, Farida Henry, Yann Leverrier, Marie Teixeira, Suzy S. Markossian, Jacqueline Marvel

► To cite this version:

Daphné Laubretton, Sophia Djebali, Céline Angleraux, Benny Chain, Maxence Dubois, et al.. Generation of a C57BL/6J mouse strain expressing the CD45.1 epitope to improve hematopoietic stem cell engraftment and adoptive cell transfer experiments. *Lab Animal*, 2023, 52 (12), pp.324-331. 10.1038/s41684-023-01275-1 . hal-04378873

HAL Id: hal-04378873

<https://hal.science/hal-04378873>

Submitted on 8 Jan 2024

HAL is a multi-disciplinary open access archive for the deposit and dissemination of scientific research documents, whether they are published or not. The documents may come from teaching and research institutions in France or abroad, or from public or private research centers.

L'archive ouverte pluridisciplinaire **HAL**, est destinée au dépôt et à la diffusion de documents scientifiques de niveau recherche, publiés ou non, émanant des établissements d'enseignement et de recherche français ou étrangers, des laboratoires publics ou privés.

Generation of a C57BL/6J mouse strain expressing the CD45.1 epitope to improve hematopoietic stem cell engraftment and adoptive cell transfer experiments

Daphné Laubretton^{1,5}, Sophia Djebali^{1,5}, Céline Angleraux², Benny Chain⁴, Maxence Dubois¹, Farida Henry², Yann Leverrier¹, Marie Teixeira², Suzy Markossian^{3,6} and Jacqueline Marvel^{1,6}

¹ CIRI, INSERM U1111, Université Claude Bernard Lyon 1, CNRS UMR 5308, École Normale Supérieure de Lyon, Université de Lyon, 69007, Lyon, France.

² SFR BioSciences, Plateau de Biologie Expérimentale de la Souris (AniRA-PBES), Ecole Normale Supérieure de Lyon, Université Lyon1, CNRS UAR3444, INSERM US8, 69007, Lyon, France.

³ Institut de Génomique Fonctionnelle de Lyon, INRAE USC 1370, CNRS UMR 5242, Ecole Normale Supérieure de Lyon, Université Claude Bernard-Lyon 1, 69007, Lyon, France.

⁴ Division of Infection and Immunity, University College London, London, United Kingdom

⁵ These authors contributed equally to the work

⁶ These authors contributed equally to the work

Corresponding author: Dr Marvel Jacqueline; e-mail: jacqueline.marvel@inserm.fr

Abstract

Adoptive cell transfer between genetically identical hosts relies on the use of a congenic marker to distinguish the donor cells from the host cells. CD45, a glycoprotein expressed by all hematopoietic cells is one of the main congenic markers used because its two isoforms, CD45.1 and CD45.2, can be discriminated by flow cytometry. As a consequence, C57BL/6J (B6; CD45.2) and B6.SJL-*Ptprc^a Pepc^b*/BoyJ (B6.SJL; CD45.1) mice are widely used in adoptive cell transfer experiments, under the presumption that they only differ at the CD45 (*Ptprc*) locus. However, recent studies identified genetic variations between these congenic strains, highlighting, among other things, a differential expression of cathepsin E (CTSE). The B6.SJL mouse presents a number of functional differences in hematopoietic stem cell (HSC) engraftment-potential and immune cell numbers. We showed that B6 and B6.SJL mice also differ in their CD8 T cells compartment and CD8 T cells responses to viral infection. We identified *Ctse* as the most differentially expressed gene between CD8 T cells of B6 and B6.SJL and demonstrated that the differences reported between these two mouse strains are not due to CTSE.

Finally, we generated a CD45.1-expressing B6 mouse by inserting one nucleotide mutation (A904G) leading to an amino acid change (K302E) in the *Ptprc* gene of B6 mouse, by CRISPR/Cas9 genome editing. We showed that this new B6-*Ptprc^{em(K302E)Jmar}*/J mouse resolves the experimental biases reported between the B6 and B6.SJL mouse lines and should thus represent the new gold standard for adoptive cell transfer experiments in B6.

Introduction

Adoptive cell transfer is a commonly used tool in the field of immunology because it allows the study of gene deletion impact on a specific cell population or to track epitope-specific T cells, such as OT-I, in a recipient mouse. This requires the use of a congenic marker that helps to distinguish donor cells from host cells. CD45 is a glycoprotein encoded by the *Ptprc* gene, located on mouse chromosome 1 and expressed by all hematopoietic cells. Its two isoforms, CD45.1 and CD45.2 can be easily distinguished by flow cytometry using anti-CD45.1 (clone A20) and anti-CD45.2 (clone 104) antibodies (Ab), making CD45 one of the main congenic markers used. The B6 (C57BL/6J) strain, which expresses the CD45.2 isoform, was crossed with the SJL mouse expressing the CD45.1 isoform to introduce the CD45.1 gene on a B6 background. The F1 hybrid was then crossed back with B6 mice for ten generations, with the selection of the CD45.1-expressing animals at each generation. The resulting congenic mouse B6.SJL (B6.SJL-*Ptprc*^{aPepc}^b/BoyCrI)²¹ was assumed to differ from B6 mouse only by the *Ptprc* gene. However, the B6.SJL mouse maintains an SJL-derived congenic interval surrounding the *Ptprc* locus, that is 27 to 72 Mb long according to the vendor source^{2,3}. Recently, the polymorphisms of SJL genes contained in this interval have been associated with experimental biases. First, the SJL congenic interval contains multiple genes that may influence hematopoietic stem cell (HSC) engraftment (e.g a polymorphism in the *CXCR4* gene)^{2,3}. As a consequence, B6.SJL HSC have a reduced engraftment potential in comparison to B6 HSC^{2,4-6}. Moreover, differences in B cells⁴, NK cells⁷ and $\gamma\delta$ T cells⁸ compartments between B6 and B6.SJL mouse have been reported. Finally, genes contained in the SJL-derived congenic interval can have different expression patterns compared to those in B6 mice. Indeed, B6 mice bear a polymorphism in the *Ctse* gene that results in the absence of cathepsin E (CTSE) expression^{3,9}, while B6.SJL mice do not. This difference has been revealed in transcriptomic analysis comparing cells purified from B6 or B6.SJL mice where *Ctse* was identified as the most differentially expressed gene³.

In this paper, we took advantage of the CRISPR/Cas9 genome editing approach to generate a new B6 mouse expressing CD45.1 epitope, by introducing point mutation(s) in B6 *Ptprc* gene using Homology Directed Repair (HDR) mechanism. We show that one mutation (A904G -> K302E) is sufficient to allow for CD45.1 epitope expression in B6 mouse. This new B6-*Ptprc*^{em(K302E)}^{Jmar}/J mouse strain shows similar hematopoietic cell composition, HSC reconstitution after transfer and similar CD8 antiviral response than B6 mouse. It thus constitutes the optimal control for comparing mutant and wild type immune cells in adoptive cell transfer experiments. Finally, as *Ctse* is one of the main differentially expressed genes between B6 and B6.SJL mice, we knocked out *Ctse* expression in B6.SJL mouse to address its role in the CD8 T cells antiviral response and HSC engraftment capacity differences reported between B6 and B6.SJL.

Results

B6.SJL differs in its CD8 T cell compartment and antiviral response as compared to B6

While the B6.SJL mouse was considered genetically and phenotypically identical to the B6 mouse, several studies have reported major differences between these two strains. Especially, it was shown that the spleen of B6 mouse was enriched in B cells as compared to B6.SJL mouse⁶. However, a detailed analysis of the T cell compartment was never performed. Thus, we compared the proportion and numbers of B and T cells in the spleen of B6 and B6.SJL mice. As expected, B cells represented a larger fraction of cells in B6 mice compared to B6.SJL. Yet, when cell numbers were compared, the spleen of B6.SJL was found to contain higher numbers of T cells, particularly CD8 T cells, as compared to B6 mice (Fig.1a-c). This results in a decrease of B-to-T cell ratio (Fig.1c). Because B6 and B6.SJL mice differ in their CD8 T cell compartment, we compared their ability to mount a memory CD8 T cell response to a viral infection. B6 and B6.SJL mice were infected with vaccinia virus (VV) and the phenotype of CD8 T cells was analyzed 31 days after infection. Similar to the non-infected mice, the VV-infected B6.SJL mice were enriched in CD8 T cells as compared to infected-B6 mice (Fig.1d-e). We first analyzed the phenotype of the CD44⁺ memory CD8 T cells and found that the fraction of cells expressing the CD62L marker or displaying the antigen-induced associated markers NKG2D¹⁰ and CD49d was higher in B6 than B6.SJL mice (Fig.1f), suggesting an increased generation of antigen-induced memory CD8 T cells¹⁰. This was confirmed by an enrichment in B8R-specific cells, as measured by B8R-tetramer staining or peptide-induced IFN γ production (Fig.1f-g).

To determine if the distinct CD8 response of B6.SJL compared to B6 mice was due to the differential expression of genes contained in the congenic interval surrounding the *Ptprc* locus^{2,3}, we compared the expression of these genes by memory CD8 T cells obtained from these two mouse lines. B6 mice were grafted with $2 \cdot 10^5$ naive F5 or F5 x CD45.1 CD8 T cells one day prior infection with *Listeria monocytogenes* (Lm). Eighty days after infection, F5 or F5 x CD45.1 memory CD8 T cells were FACS-sorted and transcriptomic analysis was performed using Affymetrix GeneChip. The *Ctse* mRNA, coding for intracellular aspartic proteinase, was the only differentially expressed gene in CD8 T cells (Fig.1h). This differential *Ctse* expression between memory CD8 T cells of B6 or B6.SJL origin was also found by others in naive and effector CD8 and CD4 T cells (<https://www.immgen.org/>) (Extended Data.Fig1). Thus, CD8 T cells generated in the B6.SJL or B6 mouse lines differ in terms of mature cell numbers generated, response to a viral challenge and in their expression of the *Ctse* gene and protein.

Generation of CD45.1-expressing B6 mice using CRISPR/Cas9 genome editing

To avoid biases associated with known or unknown polymorphisms found in B6.SJL mice, we generated a new CD45.1-expressing B6 mouse model by introducing point mutation(s) into the *Ptprc* gene of the B6 mouse. The extracellular domain sequences of the CD45.1 and CD45.2 isoforms differ by 5 nt leading to amino acid changes¹¹, which are distributed across 3 exons (Fig.2a). The K302E polymorphism in the exon 10 is referred as mutation A, the V400A, E404D and S405P polymorphisms in the exon 12 are referred as mutation B and the N478T polymorphism in the exon 14 is referred as mutation C. However, the link between each of these polymorphisms and the display of the protein epitope recognized by the anti-CD45.1 or anti-CD45.2 Ab has not been fully investigated.

In silico analysis suggests that mutation B is associated with the acquisition of the CD45.1 epitope¹¹. Furthermore, *in vitro*¹² and *in vivo*⁵ studies have shown that the introduction of mutation A leads to the expression of the CD45.1 epitope. To address the role of mutations A and B in recognition by the anti-CD45.1 antibody, we generated 3 mutant mouse models by introducing mutation A (Fig.2b), mutation B (Fig.2c) or both mutations in B6 mouse. Mutations were introduced in the *Ptprc* gene by Homology Direct Repair (HDR) using the CRISPR/Cas9 genome editing technology. Guide RNAs were selected using the CRISPOR software¹³. Template DNAs (ssODN) were designed to introduce mutation(s) of interest as well as silent mutation(s), in order to prevent a new cleavage of the mutated allele by the Cas9 nuclease (Fig.2b-c).

The resulting B6.mut^A, B6.mut^B and B6.mut^{A/B} F0 mice were backcrossed twice with their original wild-type mouse strain before the generation of homozygous lines. Sanger sequencing of PCR amplicons from mutation A (Fig.2d) and mutation B (Fig.2e) regions in homozygous mice confirmed the correct editing of the *Ptprc* sequence.

Mutation A is sufficient for the expression of the CD45.1 epitope

We then determined if the mutations introduced in the *Ptprc* gene enable the expression of the CD45.1 epitope recognized by the anti-CD45.1 Ab. Splenocytes from B6.mut^A, B6.mut^B and B6.mut^{A/B} mice were stained with anti-CD45.1 and anti-CD45.2 Ab. B6 and B6.SJL splenocytes were used as controls. We observed labelling of B6.mut^A and B6.mut^{A/B} splenocytes by the anti-CD45.1 but not the anti-CD45.2 Ab, while B6.mut^B splenocytes maintained the expression of the CD45.2 epitope (Fig.3a-b). There was no added value to introduce both mutations A and B in the *Ptprc* gene since the level of CD45.1 epitope expression was similar between B6.mut^A, B6.mut^{A/B} and B6.SJL (Figure.3b). Thus, the introduction of mutation A in the *Ptprc* gene was sufficient to generate a B6 mouse expressing the CD45.1 epitope.

It is well known that guide RNAs can bind to unintended genomic sites, potentially leading to cleavage by the Cas9 nuclease. We thus used the CRISPOR software¹³ to identify potential off-

target (OT) binding sites for mut^A guide RNA used to introduce mutation A. We selected OT sites as described in the method section. Among the 9 OT sites selected (Extended Data.Fig.2a), 2 required particular attention as they are localized on the same chromosome as the on-target, notably 1 that is located within the 20 Mb of the on-target. Among the 7 remaining selected OT sites distributed on other chromosomes, OT-mutA-3, -4, -6 and -7 sites are more susceptible to lead to Cas9 cleavage as they contain an NGG PAM sequence. The regions of potential OT sites were amplified by PCR and Sanger sequenced from the F1 mice used to amplify B6.mut^A and B6.mut^{A/B} mouse strains, with B6 mouse as control. For each OT site tested, only one fragment was amplified by PCR, with a size similar to the B6 control (Extended Data.Fig.2b). Sanger sequencing of the PCR amplicons confirmed the absence of OT cutting in B6.mut^A (Extended Data.Fig.2c) and B6.mut^{A/B} F1 mice (not shown).

A nucleotide substitution within the OT_mutA_6 sequence was observed from the provided sequence (Extended Data.Fig.2c) but trace data examination shows that it is not due to an OT cleavage but to the quality of sequencing, as chromatograms present double pics at almost each position, for B6 control and B6.mut^A mice (Extended Data.Fig.3).

B6.mut^A and B6 mice are similar in terms of B and T cell compartment generation in situ or following bone marrow transplantation

The proportion of the B and T immune cell populations was determined in the spleen of B6.mut^A mice by flow cytometry and compared to B6 and B6.SJL mice. Similar to B6 mice, B6.mut^A mice display a higher proportion of B cells and a lower proportion of T cells (both CD4 and CD8) and myeloid cells than B6.SJL mice (Fig.4a).

It is well described that B6.SJL HSC have a default in engraftment and reconstitution compared to B6 HSC^{2,4-6}. We thus evaluated the engraftment capacity of B6.mut^A HSC compared to B6 and B6.SJL HSC. Irradiated heterozygous B6/B6.SJL recipient received an equivalent number of B6.mut^A or B6.SJL and B6 bone marrow cells and the proportion of CD45.1 and CD45.2 donor cells was followed over time in the blood. An equivalent proportion of B6.mut^A and B6 donor cells was maintained in the blood of B6.mut^A/B6 chimera over time, while a defect was observed in B6.SJL donor cells compared to B6 donor cells in B6.SJL/B6 chimera (Fig.4b). After 17 weeks, the 1:1 ratio of CD45.1/CD45.2 donor cells was conserved in the spleen of B6.mut^A/B6 chimera, while it was lost in favor of B6 donor cells in B6.SJL/B6 chimera (Fig.4c-d).

There was no differences in the reconstitution of B cells, CD4 and CD8 T cells between B6.mut^A and B6 donor cells, while there was an increased proportion of T cells and a decreased proportion of B cells in B6.SJL donor cells compared to B6 donor cells (Extended Data.Fig.4). In conclusion, B6.mut^A HSC were equivalent to B6 HSC in competitive transplant assay.

B6.mut^A and B6 mice have a similar CD8 response to a viral challenge

We observed a differential CD8 antiviral response to VV between B6.SJL and B6 mice. We thus evaluated the ability of B6.mut^A mice to mount an anti-viral CD8 memory response to VV as compared to B6 and B6.SJL (Fig.5a). Thirty-one days after infection, we measured similar proportion (Fig.5b) and number (Fig.5c) of CD8 T cells in the spleen of B6.mut^A and B6 mice. In contrast, B6.SJL mice displayed higher numbers of CD8 T cells. Similar to B6 CD8 T cells, B6.mut^A memory CD8 T cells were enriched in B8R+, NKG2D+ and CD49d+ cells and displayed a lower proportion of CD62L+ cells than B6.SJL CD8 T cells (Fig.5d). Finally, we addressed the function of CD8 T cells by measuring their capacity to produce cytokines in response to B8R peptide stimulation (Fig.5e-f). A larger fraction of B6 and B6.mut^A CD8 T cells produced IFN γ , TNF α and IL-2 upon restimulation than B6.SJL CD8 T cells (Fig.5e). In conclusion, B6.mut^A mice mount an antiviral CD8 T cell response to VV that is equivalent to that of B6 mice.

Differential antiviral CD8 T cell response and HSC engraftment capacity between B6 and B6.SJL mice is not due to CTSE

We identified *Ctse* as the most differentially expressed gene between CD8 T cells from B6 and B6.SJL mice. A similar observation was made in CD4 T cells³. Indeed, the B6 mouse is naturally deficient in CTSE expression⁹. As CTSE has been implicated in antigen presentation¹⁴⁻¹⁶, we asked whether the differences we observed in CD8 T cell antiviral response between B6 and B6.SJL could be due to the recovered CTSE expression. To address this question, we generated a B6.SJL.CTSE-KO mouse by deleting 83 pb in exon 3 of the *Ctse* gene in the B6.SJL mouse using the CRISPR/Cas9 editing approach¹⁷ (Extended Data.Fig.5).

This deletion resulted in the absence of CTSE protein expression, as measured by flow cytometry in the B6.SJL.CTSE-KO mouse in comparison to the B6.SJL mouse (Fig.6a). While B6.SJL.CTSE-KO mice have slightly more B cells and CD8 T cells than B6.SJL.CTSE-WT (Fig.6b), the B/T cell ratio was comparable between B6.SJL.CTSE-KO and B6.SJL.CTSE-WT mice as compared to B6 mice (Fig.6c). Following viral infection with VV, we observed no difference in CD8 T cells proportions (Fig.6d) or numbers (Fig.6e) between B6.SJL.CTSE-KO and B6.SJL.CTSE-WT as compared to B6 mice. Furthermore, no differences were observed in CD8 T cells phenotype (Fig.6f) or ability to produce IFN γ in response to B8R stimulation (Fig.6g) between B6.SJL.CTSE-KO and B6.SJL.CTSE-WT mice.

Finally, we evaluated the impact of the absence of CTSE in hematopoietic cell reconstitution. Equivalent number of B6.SJL.CTSE-KO or B6.SJL.CTSE-WT and B6 bone marrow cells were co-transferred into irradiated heterozygous B6/B6.SJL recipients, and engraftment was followed over time in the blood. HSC from B6.SJL.CTSE-KO displayed similar defective engraftment capacity than HSC from B6.SJL.CTSE-WT, as compared to B6 HSC (Fig.6h).

Altogether, our data indicate that CTSE expression does not impact the HSC engraftment capacity and CD8 antiviral response observed in B6.SJL mice.

Discussion

In this study, we showed that the introduction of mutation A (A904G -> K302E) by CRISPR/Cas9 editing was sufficient to obtain a B6 mouse expressing the CD45.1 epitope. Unlike B6.SJL mouse, the B6.mut^A or B6-Ptprc^{em(K302E)Jmar/J} mouse differs from B6 mouse only by a point mutation in the *Ptprc* gene, thus resolving the experimental biases reported between the B6 and B6.SJL mouse lines.

The B6.SJL congenic line was generated by backcrossing SJL onto the B6 genetic background. By this method, the gene of interest is transferred to the recipient homologous chromosome by a crossing-over process that leads to the random exchange of a segment of chromatin that contains multiple genes. Despite extensive backcrossing into the B6 mouse, the B6.SJL mouse line has conserved a congenic SJL-derived interval that contains numerous genes and polymorphisms². These genetic differences are associated with functional differences between these two congenic strains. Indeed, the bone marrow HSC from B6.SJL mouse display a reduced reconstitution capacity^{2,4-6} compared to the ones from the B6 line. Moreover, the proportion of lymphoid subset B cells⁴, NK cells⁷ and $\gamma\delta$ T cells⁸ generated differs between these lines. Furthermore, we showed here that B6 and B6.SJL mice also differ in their CD8 T cells compartment. Indeed, the proportion and number of CD8 T cells were found to be lower in B6 than in B6.SJL mouse, both at a steady state or following a viral infection. However, following a viral challenge, more antigen-specific CD8 T cells were generated in the B6 line. Moreover, as it was described for CD4 T cells³, we showed that *Ctse* was the most differentially expressed gene between B6 and B6.SJL CD8 memory cells. This difference appears in public database such as Immgen (<https://www.immgen.org/>) where CD8 T cells from both B6 or B6.SJL origins were used for RNA transcriptomic analysis.

To avoid these confounding factors when performing functional or gene expression comparison between wild-type and mutant line, we generated a B6 mouse that expresses the CD45.1 epitope, using the CRISPR/Cas9 editing approach to introduce a single point mutation(s) in the *Ptprc* gene of the B6 mouse line. We showed that the introduction of the mutation A (A904G -> K302E), but not the mutation B (T1298C -> V400A; G1311T -> E404D; T1312C -> S405P) was sufficient to generate the CD45.1 epitope, thus confirming previous results^{5,12}. One major disadvantage of the CRISPR/Cas9 editing method is the potential OT cleavage by Cas9 protein due to guide RNA binding to unintended regions of the genome. During the generation of B6-Ptprc^{em(K302E)Jmar/J} mouse strain, we confirmed the absence of the most probable OT cuts linked with mutA-guide RNA. In parallel, backcrosses were performed to eliminate potential non-predicted OT cuts.

We demonstrated that B6-*Ptprc*^{em(K302E)Jmar/J} mouse has a similar hematopoietic cell composition to B6 mouse. As a consequence, B6-*Ptprc*^{em(K302E)Jmar/J} was able to elicit a CD8 T cell response to VV that was equivalent to B6 mouse. Furthermore, HSC from B6-*Ptprc*^{em(K302E)Jmar/J} mouse have similar engraftment and immune cell reconstitution potential than HSC from B6 mouse.

Mercier and colleagues developed a similar model by introducing the mutation A (A904G → K302E) in a C57BL/6N mouse, by directed mutagenesis⁵. Similar to our B6-*Ptprc*^{em(K302E)Jmar/J} mouse, their C57BL/6N-CD45.1^{STEM} mouse shows no difference in competitive transplantation experiments as compared to B6 mouse. However, C57BL/6N and B6 genome sequences differ by 34 coding SNPs and 2 coding small indels leading to significant phenotypic differences between these two strains¹⁸. Furthermore, most of mutant mice are backcrossed to B6 background. Thus, the B6-*Ptprc*^{em(K302E)Jmar/J} mouse constitutes the appropriate control for scientists working with the B6 background.

We identified *Ctse* as the most differentially expressed gene between CD8 T cells originating from B6 or B6.SJL mice. This is due to the fact that the B6 mouse strain is naturally deficient for CTSE expression due to polymorphisms in the promoter region of the gene^{3,9,19}. This leads to no or reduced CTSE expression in a number of hematopoietic lineages⁹. Many studies deciphering the role of CTSE used a CTSE-KO mouse that was generated by homologous recombination using 129 ES cells and B6 host blastocysts^{16,20}. Although this mouse model has been successfully used to describe a number of CTSE function^{15,16,20,21}, it has several limitations. First, the *Ctse* gene was knocked-out in a mouse strain that is partially deficient for this gene expression^{3,9,19}. Moreover, recent studies showed that despite backcrossing to the mouse strain of interest, mutant mice generated by homologous recombination using 129 ES cells retained some 129 genetic contents in their genome³. Therefore, to address the potential role of CTSE in the functional differences we reported between B6 and B6.SJL mice, we generated a CTSE-KO B6.SJL mouse, by CRISPR/Cas9 editing. We showed that the absence of CTSE expression has no impact on the defective engraftment capacity of B6.SJL HSC or the differential CD8 antiviral response of B6.SJL mice as compared to B6, indicating that this gene is not involved in these different functional behaviours. Additionally, the B6.SJL.CTSE-KO mouse that we generated in conjunction with the B6.SJL control constitutes a more appropriate model combination to study CTSE function, as the gene is fully expressed in the later and completely abrogated in the KO. In conclusion, our study describes a new B6 mouse line expressing the CD45.1 epitope that is suitable as a control for B6 mice in adoptive cell transfer experiments. Moreover, we describe an efficient CRISPR/Cas9 protocol to easily introduce a single point mutation in the *Ptprc* gene leading to CD45.1 epitope expression in any transgenic mouse expressing the CD45.2 isoform.

Methods

Mice

B6 (C57BL/6J), B6.SJL (B6.SJL-Ptprc^aPepc^b/BoyCrl) and B6CBAF1 (B6CBAF1/Crl) mice were purchased from Charles River Laboratories (L'Arbresle, France). F5 TCR-transgenic mice on a B6 background (B6/J-Tg(CD2-TcraF5,CD2-TcrbF5)1Kio/Jmar) were backcrossed to B6.SJL in order to obtain F5 x CD45.1 mice (B6.SJL-Ptprc^aPepc^b/BoyCrl-Tg(CD2-TcraF5,CD2-TcrbF5)1Kio/Jmar)²². The F5 TCR recognizes the (ASNENMDAM) peptide derived from the A/NT/60/68 influenza virus nucleoprotein (NP), hereafter called NP68 peptide, in the context of H2-Db. B6/B6.SJL heterozygous mice were obtained by crossing B6 with B6.SJL mice. B6.mut^A (B6-Ptprc^{em}(K302E)Jmar/J), B6.mut^B (B6-Ptprc^{em}(V400A; E404D; S405P)Jmar/J), B6.mut^{A/B} (B6-Ptprc^{em}(K302E; V400A; E404D; S405P)Jmar/J) and B6.SJL-CTSE-KO (B6.SJL-Ptprc^aPepc^bCtse^{em}(KO)Jmar/Crl)¹⁷ were generated in our animal facility (AniRA-PBES, Lyon, France). All mouse strains were housed under SPF conditions in our animal facility. Females from 6- to 12-weeks old have been used. The research projects were approved by a local ethics committee (CECCAPP, registered as CEEA-015 by the French ministry of research) and subsequently authorized by the French ministry of research. All procedures were in accordance with the European Community Council Directives of September 22, 2010 (2010/63/EU) regarding the protection of animals used for scientific purposes.

CRISPR genome editing

Guide RNAs (20 nucleotides (nt) of crRNA 5' end) design was optimized to maximize cutting specificity using the online CRISPOR software (<http://crispor.tefor.net/>)¹³. For the B6.SJL.CTSE-KO mouse generation, two guide RNAs targeting exon 3 of *Ctse* gene and allowing an 83-nt deletion were selected¹⁷. For the *Ptprc* gene point mutations, the guide RNAs with Cas9 cutting sites located as close as possible to the mutation(s) to introduce (cut-to-mutation distance < 10 nt) were selected as HDR efficiency drops with increased cut-to-mutation distance²³. In the cases where cut-to-mutation distance was superior to 10 nt, a silent mutation was added in the repair template sequence between the cutting site and the mutation to reduce this distance. 2'-O-methyl +3'phosphorothioate chemical modifications were introduced at nt 1 to 3 of crRNA and nt 69 to 71 of tracrRNA to increase guide RNA stability²⁴.

Single-stranded oligodeoxynucleotides (ssODN) used as repair templates for HDR were designed following published recommendations²⁵. Strand choice was such that ssODN sequence was complementary to guide RNA 5' end (copying the "non PAM strand"), and the position of the ssODN sequence was asymmetric with respect to the double strand break, displaced toward the 3' region. Size of 5' homology was 92 nt and 36 nt for 3' homology. Phosphorothioate modifications were introduced on the three first and three last phosphodiester bonds to protect

ssODN from nucleases²⁶. ssODN contain the mutation(s) of interest and respectively 3 or 1 silent mutation(s) within the sequence targeted by mutA-guide RNA and mutB-guide RNA, to prevent subsequent Cas-9 mediated cutting of the mutated allele. For mutation A, silent mutations created an XhoI restriction site which can be used to facilitate genotyping. Custom guide RNA and ssODN synthesis were ordered from Eurogentec with HPLC purification and PAGE purification respectively, while tracrRNA was ordered from TriLink (PAGE and HPLC purification). The RNA and DNA sequences are detailed in the Extended Datalementary Table 1.

RNP complexes composed of Cas9 protein (PNABio, #CP02), equimolar mixes of tracrRNA + guide RNA, plus or minus ssODN were prepared (respectively at 500 ng/ul, 200 ng/ul, 200 ng/ul) and zygotes from B6.SJL (B6.SJL.CTSE-KO), B6 (B6.mut^A and B6.mut^B) or B6.mut^B (B6.mut^{A/B}) were electroporated as previously described¹⁷. Embryos that reached the 2-cell stage after overnight culture were then transferred into the oviduct of B6CBAF1 pseudo-pregnant females. F0 mosaic animals were genotyped by PCR on genomic DNA extracted from toe biopsies. Point mutations were identified by Sanger sequencing of PCR products (Genewiz from Azenta life sciences). The positive F0 mice were crossed twice with original wild-type mice before the generation of homozygous mouse strains, in order to avoid possible confounding effects due to potential off-target mutations.

Off-Target mutation detection

Prediction of potential Off-Target cleavage sites (OT) were made with CRISPOR software¹³ based on sequence similarity and are listed in Extended Datalementary Fig.3. We first focused on potential OT sites localized on the same chromosome as on-target, as they can be more difficult to eliminate by backcrossing. OT sequences containing 4 mismatches compared to on-target sequences and having one or more mismatches located in PAM proximal sequence (<12 nt) were not considered as they are not likely to occur²⁷. Potential OT sites containing 3 or fewer mismatches compared to on-target were checked. Regarding potential OT localized on other chromosomes, we focused on those with up to 3 mismatches and for which all mismatches are in the PAM distal position (>12 nt), as they are more likely to occur²⁷. Potential OT mutations were determined on B6.mut^A and B6.mut^{A/B} F1 mice by Sanger sequencing of PCR products using primers listed in the Extended Datalementary Table 1.

Mouse immunization

Mice were infected by intranasal (in) instillation of a recombinant VV expressing the NP68 peptide²⁸ (VV-NP68, 2.10⁵ pfu in 20 uL) following anesthesia with ketamine/xylazine (50 and 10 mg/kg respectively injected intraperitoneally) or by intravascular (iv) administration of Listeria

monocytogenes strain 10403s expressing the NP68 peptide¹⁰ (Lm-NP, 3.10^3 pfu in 200 μ L) following brief anesthesia with isoflurane.

Transcriptomic analysis

F5 or F5 x CD45.1 memory CD8 T cells were sorted from spleen of Lm-NP infected mice. CD8 T cells were first enriched by negative selection (CD8a+ T Cell Isolation Kit, mouse, Miltenyi Biotech) on an autoMACS® Pro Separator (Miltenyi Biotech), then, memory CD8 T cells were sorted by FACS based on the expression of CD8 and CD44 (purity>98%). Total RNA was extracted from dry cell pellets using RNeasy Micro Kit (Qiagen) according to manufacturer's instruction. Purity and integrity of the RNA was assessed on the Agilent 2100 Bioanalyzer (Agilent). Total RNA from each sample was amplified, labeled, and hybridized to mouse GeneChip HT MG-430 PM Plates using Affymetrix GeneChip 39 IVT PLUS Reagent Kit (Affymetrix) according to manufacturer's instruction. Transcriptome analysis comparing F5 and F5 x CD45.1 memory CD8 T cells was conducted in R using the appropriate packages from the Bioconductor suite as previously described^{10,28}. The microarray data have been deposited to the Gene Expression Omnibus (<https://www.ncbi.nlm.nih.gov/geo/>) under accession number: [GSE86601](https://www.ncbi.nlm.nih.gov/geo/acc/show/GSE86601).

Bone marrow chimera

Donors B6, B6.SJL.CTSE-KO, B6.SJL (= B6.SJL.CTSE-WT) or B6.mut^A mice were sacrificed and bone marrow cells were isolated by flushing the femur with PBS 1X using a 23 G needle. B6/B6.SJL heterozygous recipient mice received a sublethal dose of Xray (9 Gy), 1 day prior repopulation with a 1:1 mixture of B6 and B6.SJL, B6 and B6.SJL.CTSE-KO or B6 and B6.mut^A bone marrow cells (7.10^6 cells/200 μ L).

Cell suspension preparation

Mice were sacrificed by cervical dislocation for tissue harvesting. Spleens were mechanically disrupted and filtered through a sterile 100- μ m nylon mesh filter (BD Biosciences). Femurs were flushed with PBS 1X using a 23 G needle to collect bone marrow cells. In some experiments, splenocytes were stimulated with a VV derived epitope B8R¹⁰ (TSYKFESV, 10nM) for 4h at 37 °C in the presence of GolgiStop™ (BD Biosciences) prior to intracellular staining.

Flow cytometry

Surface staining was performed on single-cell suspensions from each organ for 30 min at 4 °C with the appropriate mixture of antibody (Ab) diluted in staining buffer (PBS Extended Dataelemented with 1% FCS [Life Technologies] and 0.09% NaN₃ [Sigma-Aldrich]). For intracellular staining, cells were fixed and permeabilized using CytoFix/CytoPerm buffer

according to manufacturer's instructions (BD Biosciences) and then stained with the appropriate mixture of Ab for 30 min at 4 °C. All analyses were performed on a BD Biosciences FACS Fortessa (BD Biosciences) and analyzed with FlowJo software (Tree Star).

Statistical Analysis

Data were expressed as arithmetic median \pm range. Mann Whitney tests (comparison of two groups) was used to compare unpaired values (GraphPad Prism). Significance is represented: * $p < 0.05$ and ** $p < 0.01$.

Data availability

The mouse models will be available through EMMA (<https://www.infrafrontier.eu/emma/>) once the paper is published.

Abbreviations

Ab = Antibody

CTSE = Cathepsin E

HSC = Hematopoietic Stem Cell

nt = nucleotide

OT = Off-Target

Competing interests

The authors declare no competing interests.

Acknowledgements

We acknowledge the contribution of AniRA-Cytometrie and AniRA-PBES facilities of the SFR BioSciences (UAR3444/CNRS, US8/Inserm, Ecole Normale Supérieure de Lyon, Université de Lyon). The mice drawings in the figures were created with [BioRender.com](https://www.biorender.com) (License n°ND25XL85QU). The project was funded by the intramural CIRI grant: AO-4-2018.

Author contribution

DL, JM, SD and SM designed the study. DL, MD and SD performed the experiment. CA, FH and MT produced the mouse models. DL, JM and SM wrote the manuscript. BC and YL provided helpful discussions. SD, YL and BC reviewed the manuscript.

Bibliography

1. Shen, F. W. *et al.* Cloning of Ly-5 cDNA. *Proc. Natl. Acad. Sci.* **82**, 7360–7363 (1985).
2. Waterstrat, A., Liang, Y., Swiderski, C. F., Shelton, B. J. & Van Zant, G. Congenic interval of CD45/Ly-5 congenic mice contains multiple genes that may influence hematopoietic stem cell engraftment. *Blood* **115**, 408–417 (2010).
3. Chisolm, D. A. *et al.* Defining Genetic Variation in Widely Used Congenic and Backcrossed Mouse Models Reveals Varied Regulation of Genes Important for Immune Responses. *Immunity* **51**, 155-168.e5 (2019).
4. Basu, S., Ray, A. & Dittel, B. N. Differential representation of B cell subsets in mixed bone marrow chimera mice due to expression of allelic variants of CD45 (CD45.1/CD45.2). *J. Immunol. Methods* **396**, 163–167 (2013).
5. Mercier, F. E., Sykes, D. B. & Scadden, D. T. Single Targeted Exon Mutation Creates a True Congenic Mouse for Competitive Hematopoietic Stem Cell Transplantation: The C57BL/6-CD45.1 STEM Mouse. *Stem Cell Rep.* **6**, 985–992 (2016).

6. Jafri, S., Moore, S. D., Morrell, N. W. & Ormiston, M. L. A sex-specific reconstitution bias in the competitive CD45.1/CD45.2 congenic bone marrow transplant model. *Sci. Rep.* **7**, 3495 (2017).
7. Jang, Y. *et al.* Cutting Edge: Check Your Mice—A Point Mutation in the *Ncr1* Locus Identified in CD45.1 Congenic Mice with Consequences in Mouse Susceptibility to Infection. *J. Immunol.* **200**, 1982–1987 (2018).
8. Gray, E. E. *et al.* Deficiency in IL-17-committed V γ 4+ $\gamma\delta$ T cells in a spontaneous Sox13-mutant CD45.1+ congenic mouse substrain provides protection from dermatitis. *Nat. Immunol.* **14**, 584–592 (2013).
9. Tulone, C., Tsang, J., Prokopowicz, Z., Grosvenor, N. & Chain, B. Natural cathepsin E deficiency in the immune system of C57BL/6J mice. *Immunogenetics* **59**, 927–935 (2007).
10. Grau, M. *et al.* Antigen-Induced but Not Innate Memory CD8 T Cells Express NKG2D and Are Recruited to the Lung Parenchyma upon Viral Infection. *J. Immunol.* **200**, 3635–3646 (2018).
11. Zebedee, S. L., Barritt, D. S. & Raschke, W. C. Comparison of Mouse Ly5a. and Ly5b Leucocyte Common Antigen Alleles. *J. Immunol.* **151**, 12 (1991).
12. Kornete, M., Marone, R. & Jeker, L. T. Highly Efficient and Versatile Plasmid-Based Gene Editing in Primary T Cells. *J. Immunol.* **200**, 2489–2501 (2018).
13. Concordet, J.-P. & Haeussler, M. CRISPOR: intuitive guide selection for CRISPR/Cas9 genome editing experiments and screens. *Nucleic Acids Res.* **46**, W242–W245 (2018).
14. Chain, B. M. *et al.* The Expression and Function of Cathepsin E in Dendritic Cells. *J. Immunol.* **174**, 1791–1800 (2005).
15. Kakehashi, H. *et al.* Differential Regulation of the Nature and Functions of Dendritic Cells and Macrophages by Cathepsin E. *J. Immunol.* **179**, 5728–5737 (2007).
16. Pilzner, C. *et al.* Allergic Airway Inflammation in Mice Deficient for the Antigen-Processing Protease Cathepsin E. *Int Arch Allergy Immunol* **17** (2012).
17. Teixeira, M. *et al.* Electroporation of mice zygotes with dual guide RNA/Cas9 complexes for simple and efficient cloning-free genome editing. *Sci. Rep.* **8**, 474 (2018).
18. Simon, M. M. *et al.* A comparative phenotypic and genomic analysis of C57BL/6J and C57BL/6N mouse strains. *Genome Biol.* **14**, R82 (2013).
19. Hiramatsu, S. Regulation of Cathepsin E gene expression by the transcription factor

- Kaiso in MRL/lpr mice derived CD4⁺ T cells. 13 (2019).
20. Tsukuba, T. Association of Cathepsin E Deficiency with Development of Atopic Dermatitis. *J. Biochem. (Tokyo)* **134**, 893–902 (2003).
 21. Mengwasser, J. *et al.* Cathepsin E Deficiency Ameliorates Graft-versus-Host Disease and Modifies Dendritic Cell Motility. *Front. Immunol.* **8**, (2017).
 22. Jubin, V. *et al.* T inflammatory memory CD8 T cells participate to antiviral response and generate secondary memory cells with an advantage in XCL1 production. *Immunol. Res.* **52**, 284–293 (2012).
 23. Paquet, D. *et al.* Efficient introduction of specific homozygous and heterozygous mutations using CRISPR/Cas9. *Nature* **533**, 125–129 (2016).
 24. Hendel, A. *et al.* Chemically modified guide RNAs enhance CRISPR-Cas genome editing in human primary cells. *Nat. Biotechnol.* **33**, 985–989 (2015).
 25. Richardson, C. D., Ray, G. J., DeWitt, M. A., Curie, G. L. & Corn, J. E. Enhancing homology-directed genome editing by catalytically active and inactive CRISPR-Cas9 using asymmetric donor DNA. *Nat. Biotechnol.* **34**, 339–344 (2016).
 26. Renaud, J.-B. *et al.* Improved Genome Editing Efficiency and Flexibility Using Modified Oligonucleotides with TALEN and CRISPR-Cas9 Nucleases. *Cell Rep.* **14**, 2263–2272 (2016).
 27. Hsu, P. D. *et al.* DNA targeting specificity of RNA-guided Cas9 nucleases. *Nat. Biotechnol.* **31**, 827–832 (2013).
 28. Brinza, L. *et al.* Immune signatures of protective spleen memory CD8 T cells. *Sci. Rep.* **6**, 37651 (2016).

Figures titles/legends

Figure 1 : B6.SJL differs in their CD8 T cell compartment and antiviral response as compared to B6.

a-c, B and T cells proportions (**a**) and numbers (**b**) were measured in the spleen of B6 and B6.SJL mice and B/T ratio (**c**) was determined. **d-g**, B6 and B6.SJL mice were infected intranasally with VV ($2 \cdot 10^5$ pfu/mouse) and the proportion (**d**) and the numbers (**e**) of CD8 T cells were measured in the spleen 31 days after infection. The CD8 T cells phenotype was analysed by flow cytometry (**f**). The production of IFN γ in response to stimulation with B8R peptide was measured by flow cytometry (**g**). **h**, Congenic interval as described by (Waterstrat et al., 2010) was analysed by transcriptomic analysis for F5 x CD45.1 and F5 purified CD8 memory cells and differential gene expression was represented as a heatmap. Results are expressed as the median \pm range (n = 5-8 mice/group, one out of three representative experiments). The statistical significance of differences was determined by Mann-Whitney test (*p<0.05, **p<0,01).

Figure 2 : Mutation of Ptpcr gene by CRISPR/Cas9 editing for the expression of CD45.1 epitope in B6 mouse

a, Alignment of B6 (CD45.2) and B6.SJL (CD45.1) *Ptpcr* genomic sequences. CD45.1 and CD45.2 extracellular domain sequences differ by 5 nt leading to amino acid changes located in three exons. **b-c**, Mutation A (**b**) and mutations B (**c**) targeted sequences. Sequence targeted by the guide RNA is underlined, sequence covered by the ssODN is bolded and nucleotides to be mutated are in lower case letters (red for mutations of interest, blue for silent mutations). PAM and cutting site (represented by /) are in orange and PCR primers are shaded. **d-e**, Sanger sequencing of mutation A (**d**) and mutation B (**e**) loci for B6.mut^A, B6.mut^B, B6.mut^{A/B} and B6 mice. Mutated nucleotides are highlighted (red arrow for mutations of interest, blue for silent mutations).

Figure 3 : Mutation A but not mutation B is necessary for CD45.1 epitope expression

The expression of the CD45.1 and CD45.2 epitopes was analysed by flow cytometry on splenocytes from B6.mut^A, B6.mut^B, B6.mut^{A/B}, B6 and B6.SJL mice. **a**, Representative dot plots of CD45.1 and CD45.2 epitope expression are represented for all mouse strains. **b**, MFI of CD45.1 and CD45.2 epitope expression were determined. Results are expressed as the median \pm range (n = 4-5 mice/group, one out of two representative experiments).

Figure 4 : B6.mutA and B6 have similar hematopoietic cell compartment before and after transplantation

a, Hematopoietic cell compartment was analysed by flow cytometry in the spleen of B6.mut^A, B6 and B6.SJL mice. Percentages of cells were determined. **b-c**, Irradiated B6/B6.SJL heterozygous mice received a 1:1 mixture of B6.mut^A or B6.SJL and B6 bone marrow cells. **b**, CD45.1 and CD45.2 donor cell engraftment was followed over time in the blood by flow cytometry. **c**, CD45.1/CD45.2 ratio was determined in the blood and spleen, 17 weeks after transfer. Results are expressed as the median \pm range

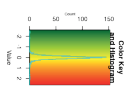
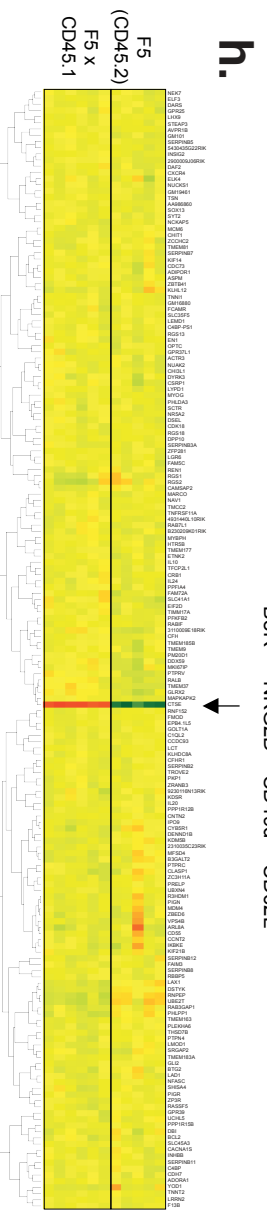
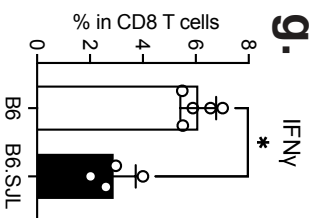
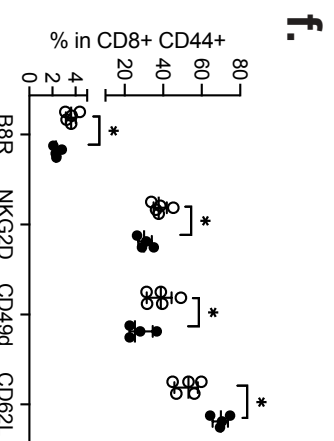
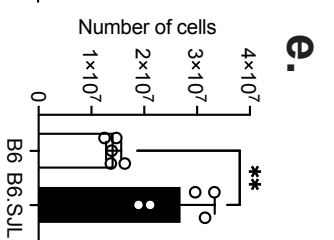
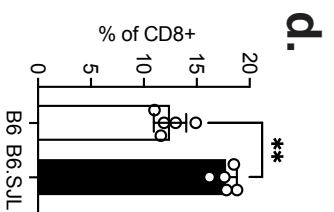
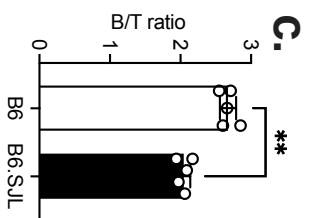
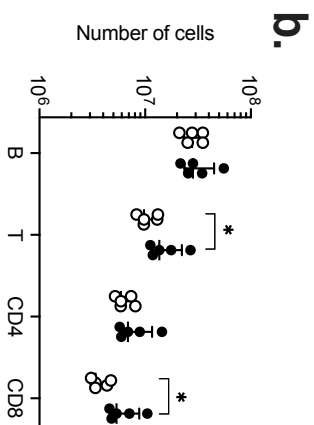
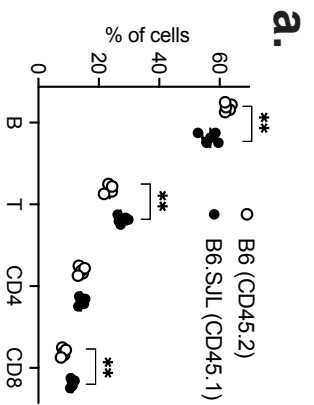
(n = 5 mice/group, one out of three representative experiment). The statistical significance of differences was determined by Mann-Whitney test (*p<0.05, **p<0,01).

Figure 5 : B6.mut^A mice have a similar antiviral CD8 response to VV than B6 mice

a. B6.mut^A, B6 or B6.SJL were infected in with VV (2.10^5 pfu/mouse) and spleens were collected 31 days after infection. **b-c**, Percentages (**b**) and number (**c**) of CD8 T cells were determined. **d**, Proportions of CD8 T cells positive for B8R, NKG2D, CD49d and CD62L markers were measured. **e-f**, Splenocytes were stimulated with B8R peptide for 4 hours in the presence of Golgi Stop, and the expression of IFN γ , TNF α and IL-2 was measured by flow cytometry (**e**). Results are expressed as the median \pm range (n = 5 mice/group, one of three representative experiments). The statistical significance of differences was determined by Mann-Whitney test (*p<0.05, **p<0,01).

Figure 6 : Differential antiviral CD8 T cell response and HSC engraftment capacity between B6 and B6.SJL mice is not due to CTSE

a, CTSE expression was determined in the blood of B6, B6.SJL.CTSE-WT and B6.SJL.CTSE-KO mice by flow cytometry. **b-c**, B and T cells proportions (**b**) were measured in the spleen of B6, B6.SJL.CTSE-WT and B6.SJL.CTSE-KO mice and B/T ratio was determined (**c**). **d-h**, B6, B6.SJL.CTSE-WT and B6.SJL.CTSE-KO mice were infected with VV and the proportions (**d**) and numbers (**e**) of CD8 T cells was measured in the spleen 30 days after infection. The CD8 T cells phenotype was analysed by flow cytometry (**f**). The production of IFN γ in response to stimulation with B8R peptide was measured by flow cytometry (**g**). **h**, Irradiated B6/B6.SJL heterozygous mice received a 1:1 mixture of B6.SJL.CTSE-WT or B6.SJL.CTSE-KO and B6 bone marrow cells. CD45.1 and CD45.2 cell engraftment was followed over time in the blood by flow cytometry. Results are expressed as the median \pm range (n = 5 mice/group, one of two representative experiments). The statistical significance of differences was determined by Mann-Whitney test (*p<0.05, **p<0,01).



a.

Exon 10
 K302E A904G
 GGCTAATACTTCAATTTGTTTGGAGTGGAAAACA**A**AAAACCTTGATTTTCAGAAAATGCAA **B6 (CD45.2)**
 GGCTAATACTTCAATTTGTTTGGAGTGGAAAACA**G**AAAACCTTGATTTTCAGAAAATGCAA **B6.SJL (CD45.1)**
Mutation A

Exon 12
 V400A E404D S405P
 T1298C G1311T T1312C
 CGTTAGTCTCTTGGCCTGAGCCTG**T**ATCTAAACCTGAG**T**CTGCATCTAAACCCCATGGAT **B6 (CD45.2)**
 CGTTAGTCTCTTGGCCTGAGCCTG**C**ATCTAAACCTG**T**CTGCATCTAAACCCCATGGAT **B6.SJL (CD45.1)**
Mutation B

Exon 14
 N478T A1532C
 ACAAGGTCA**A**TGGAATGAAAACCTCCCGGCCGACAGACAATAGTAT **B6 (CD45.2)**
 ACAAGGTCA**C**TGGAATGAAAACCTCCCGGCCGACAGACAATAGTAT **B6.SJL (CD45.1)**
Mutation C

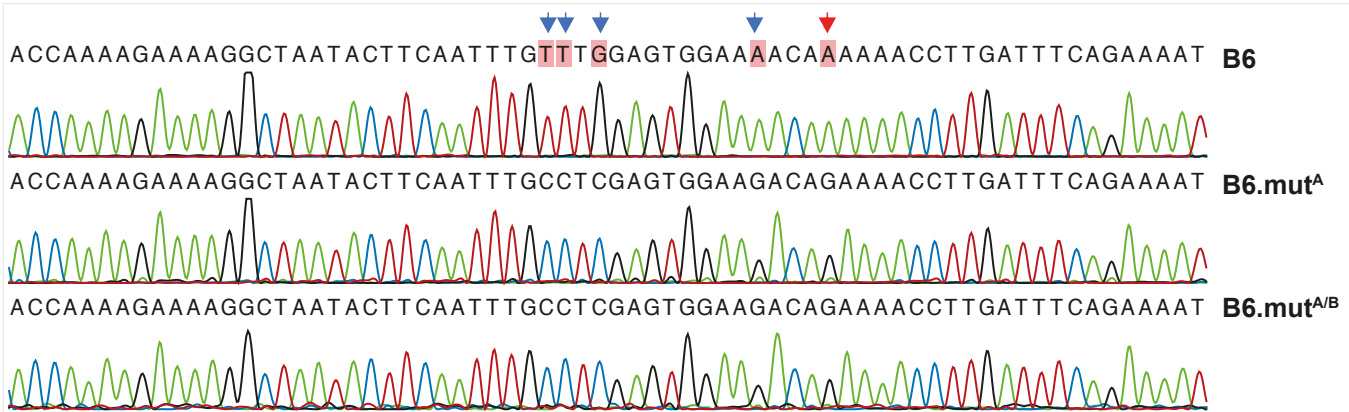
b.

CATGAAGAAGCATCAGACCTTGGGAGAGCTTAGATGTCCCTAGCGAAATCTCCTGCTTGCAGACTGTACTCCATGAGTCT
 TATTTTCAGAGTTGAGAGGGTTCACATCTCCACACCAGGAACCATCACCTAAGAGCACCTCTCCGTTTCCCTCCACAGGGACTG
 ACAAGTTTTTCGCTACATGACTGCACACCAAAAGAAAAGGCTAATACTTCAATTTG**ttTg**/**GAGTGGAAaACAa**AAAACCTTG
ATTTTCAGAAAATGCAACAGTGACAATATTTTCATATGTACTCCACTGTGAGCCAGGTACGATGCTGGGCAGAGAAGTTCTATT
 ATCAGAAATTATTCCAGACGTGGCTTAAATGTTCTTTCTGTAGCCTTGTCCCTCACCCACCCTCAGTGATCCGCCATAAA
 TTAGAATAAAAATAACCCTAGTATCTCTGGCACTGAAACAAAATTCACAACGTAGATAAATGAAAAGAGCAACCCATGGATGAT
 AAATATTATGAAAAATTAATTAAGAATTTTCTTGAGTACTGTTATATACCAGACATTGTTGAAAGGGTGATGAGATGCAG
 GCATTATAAAAAGAAAGATGGTATCCATAGTCTGTAGAAAGGAAGCATAGTATTATCCACACCGGAGGTTGCTTTCTCAG

c.

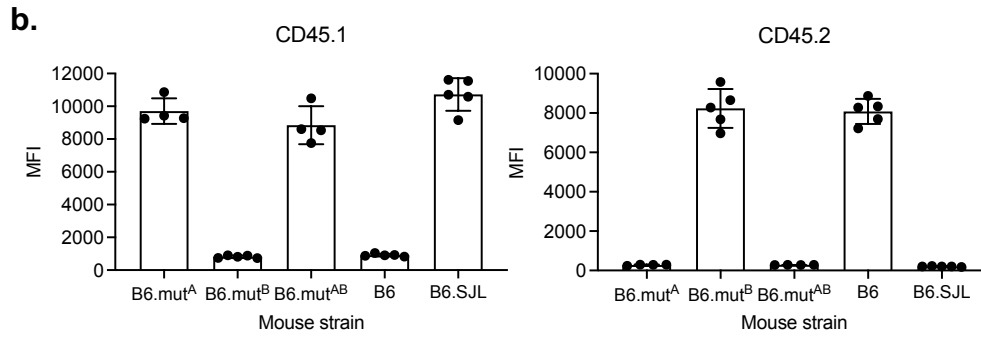
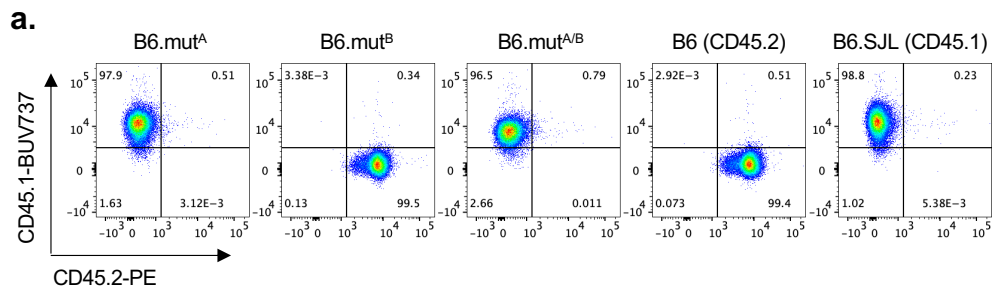
ATTATTGGGTAGTCTTCAGATCAGTGGGATAACTAGCCAAAAAGAATCTATGAAAGAAATCTAATCTAAATGATCCAGGATA
 GGTCTAAGAACTTCACTGAGATTTTATTAATTCACAATTAATCAAAAGATAGGTATTCATGATTCAAGCTGGCTATGTAAT
 ACTTCTTTTTCAGTGTCTTATTTTCCATTATAACTTTTCTGTTTTTTAACAGTTCCAGAAACGCCTAAGCCTAGTTGTGGG
GATCCAGCTGCAAGAAAAACGTTAGTCTCTTGGCCTGAGCCTGtA/TCtAAACCTGAgtCTGCATCTAAACCCCATGGATAT
GTTTTATGCTATAAAGAACAATTCAGGTAATGTAAAATTCCACTAGGGAAACAAAATCAAGAATTTTTAAATGTTGTAATTAT
 TGTTTTAGCCAGGGAGCTACAAGGCTTTTATGAAGGTGATGAGAGATTCATGTTTGAGTTTGCTTAGATGAACACGCATCTC
 ATGGAGAAGAATAAATATCTAGATCATTATTAATAAATAGTGGACAGGACTAGAGTCCTTTA

d.

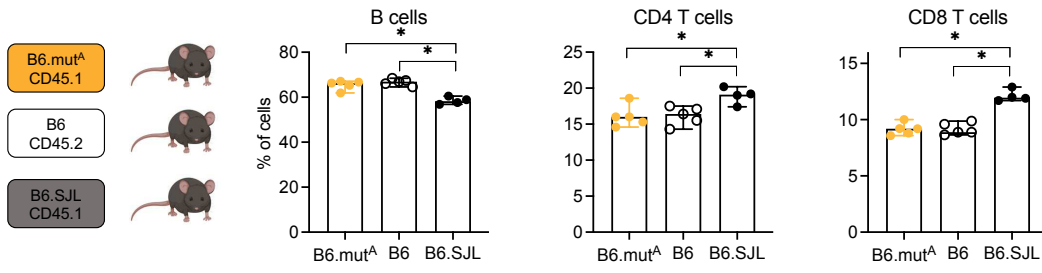


e.

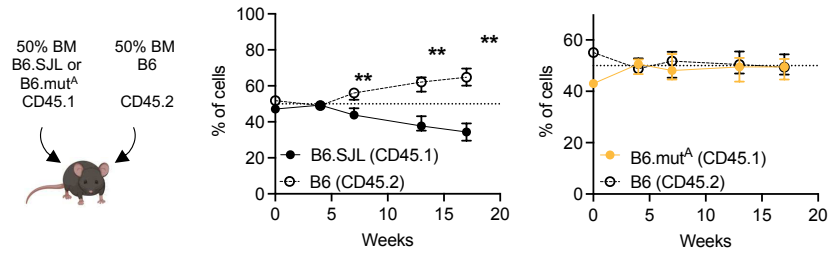




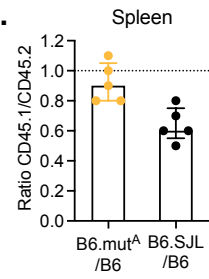
a.



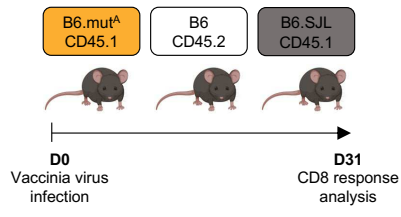
b.



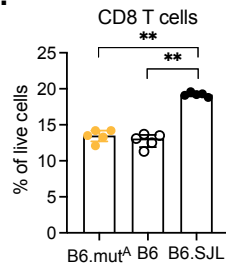
c.



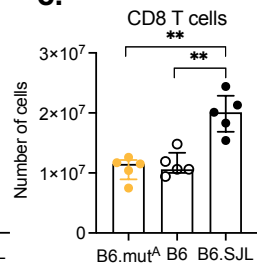
a.



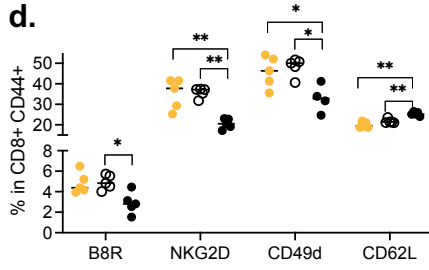
b.



c.



d.



e.

